

# Cripto recruits Furin and PACE4 and controls Nodal trafficking during proteolytic maturation

Marie-Hélène Blanchet<sup>1,4</sup>, J Ann Le Good<sup>1,4</sup>, Daniel Mesnard<sup>1</sup>, Viola Oorschot<sup>2</sup>, Stéphane Baflast<sup>1</sup>, Gabriella Minchiotti<sup>3</sup>, Judith Klumperman<sup>2</sup> and Daniel B Constam<sup>1,\*</sup>

<sup>1</sup>Ecole Polytechnique Fédérale de Lausanne (EPFL), and Swiss Institute for Experimental Cancer Research (ISREC), Epalinges, Switzerland,

<sup>2</sup>Department of Cell Biology, Cell Microscopy Center, Utrecht,

The Netherlands and <sup>3</sup>Institute of Genetics and Biophysics

'A Buzzati-Traverso', Naples, Italy

**The glycosylphosphatidylinositol (GPI)-anchored proteoglycan Cripto binds Nodal and its type I receptor Alk4 to activate Smad2,3 transcription factors, but a role during Nodal precursor processing has not been described. We show that Cripto also binds the proprotein convertases Furin and PACE4 and localizes Nodal processing at the cell surface. When coexpressed as in early embryonic cells, Cripto and uncleaved Nodal already associated during secretion, and a Cripto-interacting region in the Nodal propeptide potentiated the effect of proteolytic maturation on Nodal signalling. Disruption of the trans-Golgi network (TGN) by brefeldin A blocked secretion, but export of Cripto and Nodal to the cell surface was not inhibited, indicating that Nodal is exposed to extracellular convertases before entering the TGN/endosomal system. Density fractionation and antibody uptake experiments showed that Cripto guides the Nodal precursor in detergent-resistant membranes to endocytic microdomains marked by GFP-Flotillin. We conclude that Nodal processing and endocytosis are coupled in signal-receiving cells.**

*The EMBO Journal* (2008) 27, 2580–2591. doi:10.1038/emboj.2008.174; Published online 4 September 2008

**Subject Categories:** membranes & transport; development

**Keywords:** EGF-CFC; TGFβ; trafficking; unconventional exocytosis

## Introduction

In early vertebrate embryos, the fate of pluripotent cells is dictated by Nodal proteins through complexes of Alk4 and activin type II receptors (ActRII) (reviewed in Shen, 2007). Alk4 mediates Nodal activities in the mouse embryo by stimulating phosphorylation and nuclear translocation of the transcription factors Smad2 and 3. Nodal is secreted

as a precursor protein, which must be cleaved to induce mesendodermal genes and gastrulation movements within the epiblast (Brennan *et al*, 2001; Beck *et al*, 2002; Guzman *et al*, 2004; BenHaim *et al*, 2006). Genetic and biochemical evidence suggests that Nodal is processed by the secreted proprotein convertases (PCs) Furin and PACE4 (Beck *et al*, 2002), but how this interaction is regulated is unknown. Whereas Nodal is secreted by epiblast cells, Furin and PACE4 are provided by neighbouring cells in the extraembryonic ectoderm (Beck *et al*, 2002; Mesnard *et al*, 2006). Therefore, we hypothesized that secreted forms of Furin and PACE4 activate Nodal in extracellular fluid, or that they are recruited to an unknown receptor in target cells.

In cell-free assays, Nodal can be processed by soluble Furin and PACE4 (Beck *et al*, 2002; Mesnard *et al*, 2006), but removal of the N-terminal propeptide in tissue culture promotes endocytosis and turnover (Constam and Robertson, 1999; Le Good *et al*, 2005). In zebrafish, rapid clearance of mature Nodal, rather than proteolytic processing, seems to limit its signalling range (Constam and Robertson, 1999; Le Good *et al*, 2005). Thus, we hypothesized that to efficiently signal, Nodal may have to mature in a privileged compartment in signal-receiving cells.

To activate Alk4/Smad2,3 signalling, Nodal also depends on glycosylphosphatidylinositol-anchored proteins (GPI-AP) of the EGF-CFC proteoglycan family, such as Cripto (Ding *et al*, 1998; Gritsman *et al*, 1999; Reissmann *et al*, 2001; Schier, 2003). Biochemical analysis has shown that Cripto independently binds both Alk4 and Nodal, or the related ligands Gdf1 or -3 (Reissmann *et al*, 2001; Cheng *et al*, 2003; Schier, 2003; Chen *et al*, 2006). However, in cell-free assays and at the surface of cultured cells, Nodal can bind ActRII and Alk4 independently of Cripto (Reissmann *et al*, 2001; Chen and Shen, 2004; BenHaim *et al*, 2006). Furthermore, Nodal clearly retains significant activity in Cripto<sup>-/-</sup> mice (Ding *et al*, 1998), which can be further enhanced by inactivating the feedback inhibitor Cerl (Liguori *et al*, 2008). Similarly in zebrafish, loss of zygotic expression of the Cripto homologue Oep can be partially rescued by eliminating the small GTPase Rasl11b/RLP, a novel feedback inhibitor of maternal Nodal/Oep and other Smad-mediated TGFβ and BMP signals (Piek *et al*, 2004; Pezeron *et al*, 2008). Thus, Cripto may be required to antagonize context-dependent, inhibitory mechanisms.

Owing to their membrane anchor, GPI-APs can recruit cargo to microdomains known as lipid rafts and access early endosomes by clathrin- and Caveolin-independent carriers (Stuermer *et al*, 2001; Fivaz *et al*, 2002; Sabharanjak *et al*, 2002). Therefore, we hypothesized that besides its known functions, Cripto also regulates Nodal trafficking. Here, we report that Cripto and Nodal use an unconventional exocytic pathway and recruit extracellular Furin, and that Cripto localizes Nodal processing to promote endocytosis in membrane carriers that overlap with the raft scaffold protein Flotillin. On the basis of these results, we propose that in addition to its known functions, Cripto targets

\*Corresponding author. Ecole Polytechnique Fédérale de Lausanne (EPFL), Swiss Institute for Experimental Cancer Research (ISREC), 155, Chemin des Boveresses, S/Lausanne, 1066 Epalinges, Switzerland. Tel.: +41 21 692 5820; Fax: +41 21 652 6933;

E-mail: daniel.constam@epfl.ch

<sup>4</sup>These authors contributed equally to this work

Received: 7 March 2008; accepted: 8 August 2008; published online: 4 September 2008

the assembly of a Nodal-processing complex to specific membrane microdomains.

## Results

### **Processing and secretion of Nodal and Cripto**

To characterize trafficking, we first determined how Nodal is modified during exocytosis. Western blot analysis of transfected cells showed that incubation with endoglycosidase H (EndoH) or *N*-glycosidase F shifted the molecular weight of intracellular Nodal from 42 to 39 kDa, the predicted size of unmodified precursor. In contrast, the 47 kDa Nodal precursor and propeptide (35 kDa) in conditioned medium were sensitive to *N*-glycosidase F and neuraminidase, but not to EndoH, indicating that they acquired complex carbohydrates in the trans-Golgi network (TGN) (Figure 1A).

We also monitored processing of Cripto. Cripto is tethered to membranes through a GPI anchor (Kenney *et al*, 1996; Minchiotti *et al*, 2001). The predicted molecular weight of full-length Cripto is 18 kDa, but a prosegment is cleaved after proline 52 (Kenney *et al*, 1996; Minchiotti *et al*, 2001). Incubation of cell extracts with EndoH or *N*-glycosidase F, or inhibition of *N*-glycosyltransferases in the ER by tunicamycin shifted the 18-kDa form of Cripto to 13 kDa (Figure 1B). This suggests that Cripto is cleaved before entering the Golgi apparatus.

Immunostaining of transfected cells revealed that Cripto and Nodal colocalize with the ER marker RFP-KDEL in a reticular network (Supplementary Figure S1). To assess how Cripto is secreted, we analysed the effect of brefeldin A (BFA), a compound that blocks ER to TGN transport. Western blot analysis revealed that BFA blocked the secretion of Cripto into the medium (Figure 1C). However, immunostaining of unpermeabilized cells showed that Cripto levels at the cell surface were unaffected, except when BFA was added together with cycloheximide to block protein synthesis (Figure 1C, right panel). These results suggest that newly synthesized Cripto is exported to the plasma membrane independently of the TGN, whereas the TGN mediates terminal glycosylation and secretion of Cripto into the medium.

To validate this conclusion, we also monitored the secretion of mutant Cripto carrying a 6 × His tag instead of the GPI signal sequence (CriptoHis). CriptoHis is secreted, and complex carbohydrates shift the molecular weight to approximately 29 kDa (Kenney *et al*, 1996; Minchiotti *et al*, 2001). By contrast, in cells treated with BFA, CriptoHis was shifted to 24 kDa and was not secreted into the medium (Figure 1D). CriptoHis cannot be tethered to the plasma membrane by a GPI anchor, but may still bind to receptors (Bianco *et al*, 1999; Yan *et al*, 2002). Indeed, immunofluorescent staining detected significant amounts of CriptoHis at the cell surface, which were reduced to background levels by BFA (Figure 1D). BFA also inhibited the cell surface expression of secreted GPI-anchored eGFP (Figure 1E), and was not toxic during the time window examined. These data confirm that BFA efficiently blocked TGN-mediated exocytosis, but that wild-type Cripto through its GPI signal uses a BFA-insensitive route to reach the plasma membrane.

### **Cripto intercepts the Nodal precursor during exocytosis**

As a first step to test whether Cripto affects Nodal processing, wild-type Nodal or cleavage-resistant mutant precursor was

co-transfected with increasing doses of Cripto. Cripto dose-dependently inhibited the release of the 47-kDa form of wild-type Nodal precursor into the medium. This effect was specific in that the PC-resistant mutant Nodal was barely affected by Cripto (Figure 2A, Nr). Conversely, secretion of Cripto was not diminished, but rather increased in cells coexpressing Nodal (data not shown), suggesting that non-specific trapping in the ER is unlikely. In contrast to wild-type Cripto, CriptoHis did not diminish the secretion of Nodal into the medium (Figure 2B). These results suggest that the mechanism leading to sequestration of the Nodal precursor involves GPI anchoring of Cripto and PC-mediated processing.

A common feature of GPI-anchored proteins is their localization in lipid rafts. To assess whether Cripto recruits the Nodal precursor to rafts, detergent lysates of transfected cells were fractionated by density gradient centrifugation. In the absence of Cripto, Nodal was detected exclusively in its uncleaved form in high-density fractions 5 and 6, together with the transferrin receptor. By contrast, when co-transfected with Cripto, a significant amount of uncleaved Nodal partitioned to the detergent-resistant membrane fraction 1 (Figure 2C). To determine whether the amount of Nodal precursor entering lipid rafts might be underestimated due to proteolytic processing and subsequent degradation, we also fractionated cells expressing the cleavage mutant precursor Nr. Interestingly, Nr and a degradation intermediate appeared in fraction 1 even in the absence of Cripto, and this amount consistently increased in cells expressing Cripto (Figure 2D). The molecular weight of Nodal in fraction 1 was 42 kDa, corresponding in size to EndoH-sensitive precursor (cf. Figure 1A), whereas the secreted 47-kDa isoform was only detected in fractions 5 and 6 even after prolonged exposure (Figure 2D, and data not shown). Taken together, these results indicated that the pre-TGN 42-kDa isoform of Nodal precursor is intercepted by Cripto before PC-mediated processing and sorted to specific membrane microdomains.

### **The Nodal precursor reaches the cell surface via a TGN-independent route**

Generally, PCs must enter acidic compartments to dissociate from their inhibitory propeptides (Chapman and Munro, 1994; Mallet and Maxfield, 1999; Anderson *et al*, 2002; for review, see Thomas, 2002), and endosomal acidification is also required to release Furin and PACE4 into culture medium (Supplementary Figure S2). If these proteases must pass the TGN/endosomal system to become active, how can they cleave the pre-TGN isoform of Nodal and reduce its accumulation in lipid rafts? Precocious activation of endogenous PCs in the ER is unlikely, given the absence of intracellular cleavage products. To resolve this paradox, we hypothesized that Nodal bypasses the TGN and is directly targeted to the cell surface to recruit PCs from the extracellular space. Indeed, examination of chemically crosslinked cell surface complexes suggests that Nodal and Cripto proteins at the cell surface correspond in size to the EndoH-sensitive isoform (Yan *et al*, 2002; Chen and Shen, 2004; BenHaim *et al*, 2006). Furthermore, glycan maturation and secretion of the 47-kDa form of Nodal into the medium were inhibited by NH<sub>4</sub>Cl and chloroquine (Supplementary Figure S2). These data pointed towards an unconventional exocytic pathway, involving perhaps endosomal uptake to release Nodal into the medium.

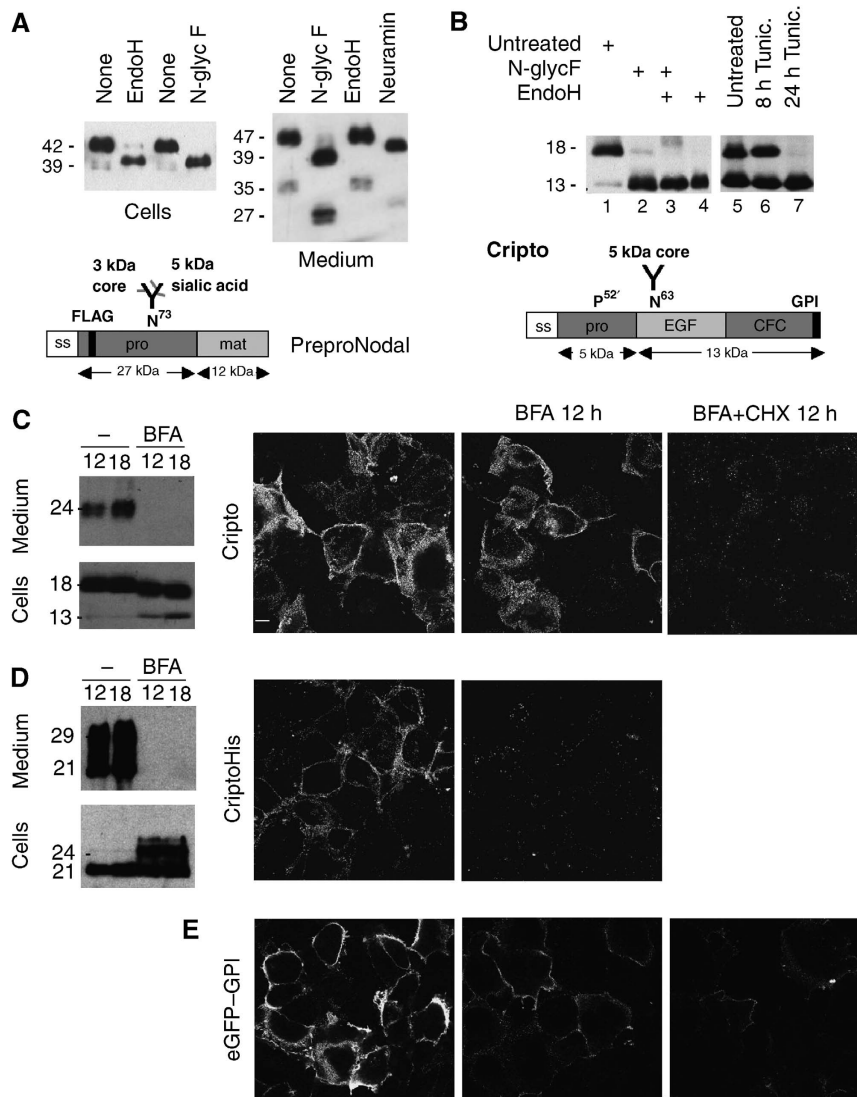


**Figure 1** Post-translational modifications of Nodal and Cripto. **(A)** Western blot of Nodal in lysates (left) and conditioned medium (right) of transfected COS1 cells. Treatment with EndoH or *N*-glycosidase F shifted the size of intracellular Nodal from 42 to 39 kDa, the predicted molecular weight of unmodified precursor. In conditioned medium, precursor and Nodal propeptide (47 and 35 kDa) were sensitive to *N*-glycosidase F and neuraminidase, but not to EndoH. Bottom: impact of processing on the size of Nodal. **(B)** Western blot analysis of Cripto in COS1 cell lysates before and after treatment with *N*-glycosidase F, EndoH or both, or after incubation of cells with tunicamycin. Processed Cripto lacking the N-terminal 52 amino acids (Minchiotti *et al*, 2001) has a predicted size of 13 kDa, but migrates at an apparent molecular weight of 18 kDa due to high mannose *N*-glycosylation. **(C)** Left: truncated mutant Cripto lacking a GPI signal (CriptoHis) is shifted in size to 29 kDa by complex carbohydrate modifications (Minchiotti *et al*, 2001), and its release into conditioned medium is blocked by BFA. Right: also shedding of wild-type Cripto is abolished in the presence of BFA. **(D)** Immunostaining of unpermeabilized COS1 cells shows that BFA blocks the expression of CriptoHis at the cell surface, but not that of wild-type Cripto. **(E)** Cripto staining at the surface of unpermeabilized cells is blocked in cells where BFA was administered together with cycloheximide.

To directly test whether Nodal bypassed the TGN, cells expressing Nr with or without Cripto were incubated with fresh medium containing BFA. Immunofluorescence and western blot analysis revealed that BFA did not diminish Nr staining at the surface of unpermeabilized cells, except when added together with cycloheximide (Figure 3A). However, BFA abolished the secretion of the soluble 47-kDa isoform into culture medium (Figure 3B). Under these conditions, the 47 kDa precursor ectopically accumulated in cell lysates (Figure 3B), indicating that Nodal is internalized in the BFA compartment containing sialyltransferases that are shunted from the TGN to endosomes (Nebenfuhr *et al*, 2002). Importantly, BFA also inhibits the secretion of Furin (Supplementary Figure S3A). To eliminate the confounding

influence of PC-mediated cleavage on Nodal expression levels, these experiments were conducted using cleavage-resistant precursor (Nr), but analogous results were obtained for cleavable Nodal (Supplementary Figure S3B and C). We conclude that BFA selectively blocks secretion into the medium, but that Nodal export to the cell surface is TGN independent.

#### **Cripto independently interacts with processed Nodal and its pro peptide**

To test whether Nodal binds Cripto before proteolytic maturation, a mixture of soluble Nodal propeptide, mature form and residual uncleaved precursor (Figure 4A, top panels) was incubated with metal agarose beads soaked with or without

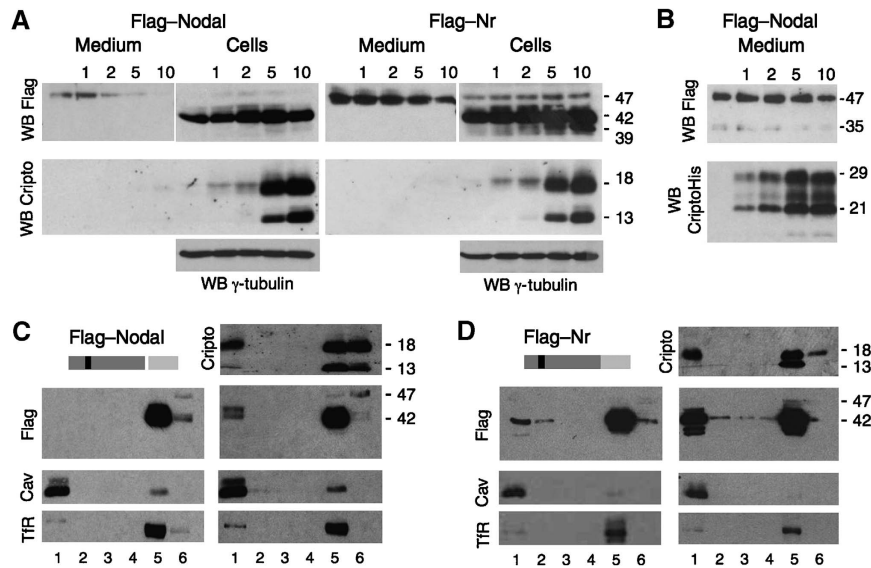


**Figure 2** GPI-anchored Cripto intercepts the Nodal precursor in lipid rafts. **(A)** In co-transfection assays, Cripto dose-dependently reduces the amount of soluble Flag-tagged Nodal precursor (47 kDa) in conditioned medium (top left panels). Compared with wild-type Nodal, mutant precursor lacking the PC cleavage site (Nr, right panels) is more resistant to Cripto-induced turnover. Bottom panels: GPI-anchored Cripto accumulated in cell lysates. After prolonged exposure, Cripto is also detected in conditioned medium (not shown). The anti-Flag western blot of cell lysates is overexposed to detect fully modified Nodal precursor (47 kDa). **(B)** Truncated Cripto lacking the GPI anchor (CriptoHis) is released without affecting Nodal. The Nodal propeptide (35 kDa) can be detected in small amounts in conditioned medium, but is below detectable levels in cell lysates (Constam and Robertson, 1999). All results are representative of more than three independent experiments, and the amount of transfected DNA including empty vector in all transfections was 10  $\mu$ g.  $\gamma$ -Tubulin staining served as a loading control. **(C, D)** Western blots of detergent extracts of transfected cells fractionated in OptiPrep density gradients. In fraction 1 (lipid rafts), Cripto increases the amount of pre-TGN wild-type precursor (42 kDa) and Nr (right panels in C and D, respectively). The distribution of Cripto was not altered in the absence of Nodal (data not shown). Nr was detected in fraction 1 together with a breakdown product (37 kDa) even in the absence of Cripto (left panels in C and D). Separation of lipid rafts from detergent-soluble proteins was confirmed by re-probing the blots with anti-Caveolin-1 (Cav) and transferrin receptor (Tfr) antibodies. All results are representative of at least three independent experiments.

CriptoHis. CriptoHis mainly pulled down uncleaved Nodal (top panels), despite a molar excess of processed Nodal and propeptide in the input (bottom panels). However, when incubated with Nodal-sc, which is more efficiently processed due to a mutant cleavage site (Constam and Robertson, 1999), CriptoHis pulled down both mature Nodal and propeptide (lane 2). These results indicate that Nodal binds Cripto before and after proteolytic maturation.

To validate this conclusion, wild-type Cripto was solubilized and coimmunoprecipitated with Flag-tagged Nodal proteins from cell extracts. The 42 kDa Nodal precursor precipitated both the 18- and 13-kDa forms of Cripto (Figure 4B, lanes 1 and 2). Cripto also precipitated with constitutively mature mutant Nodal (Nmat, lane 4) fused directly to a secretory signal sequence (Le Good *et al*, 2005). We also detected a complex of Cripto with Nodal propeptide (Npro) alone, although it was less soluble and in lipid rafts (lane 2, and data not shown). This interaction was confirmed using Npro fused to GFP as a substitute for mature domain (Figure 4C). In control experiments, Cripto was not precipitated by the TGF $\beta$  family member Dorsalin (data not shown). Thus, wild-type Cripto and CriptoHis specifically bind uncleaved Nodal both through the mature domain and the pro segment.

#### **A Cripto-interacting region in the Nodal propeptide potentiates signalling**

Next, we mapped a Cripto-interacting region (CIR) in the Nodal propeptide and tested whether it is necessary to

activate Nodal. Residues 215–226 of the Nodal propeptide are highly conserved in other TGF $\beta$ s that bind Cripto (Figure 4D), but deletion of this motif in Npro-GFP was not sufficient to abrogate Cripto binding (data not shown). To test whether they comprise a CIR, residues 203–229 of Nodal were fused to secreted CFP. Coimmunoprecipitation analysis showed that this fragment was sufficient to bind Cripto (Figure 4E). Mutation of four amino acids of the CIR, including L216 and S223, diminished this interaction in three out of three experiments (ssCFP-CIRmut; Figure 4D and F), suggesting that they contribute to Cripto binding.

To assess whether the CIR regulates Nodal signalling, it was mutated in the Nodal precursor. Western blot analysis showed that the CIR is not required for protein folding, secretion or Cripto-independent maturation (Figure 4G). Nevertheless, mutation or deletion of the CIR reduced Cripto-mediated Nodal signalling more than 2.5-fold (Figure 4G). Mutation of the CIR also inhibited paracrine signalling of secreted Nodal/Cripto in cell mixing assays (Figure 4H). Taken together, these results confirm that even though Cripto-independent Nodal cleavage can occur extracellularly, processing without the CIR does not efficiently stimulate signalling.

#### **Cripto binds the Nodal convertases Furin and PACE4**

As Cripto associates with uncleaved Nodal precursor, we asked whether it also recruits PCs. Immunoprecipitation revealed that both Flag-tagged Furin and PACE4 can pull down Cripto and vice versa (Figure 5A and B). Deletion of

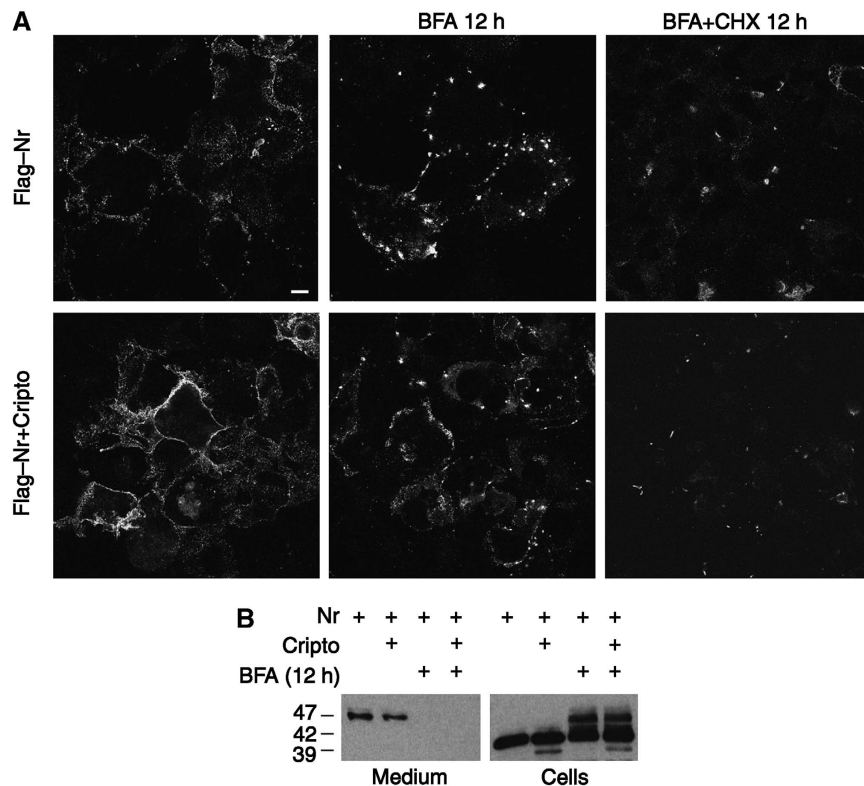


**Figure 3** Transport through the TGN/endosomal system is essential for the secretion and processing of Nodal precursor, but not for cell surface expression. (A) Immunostaining of Flag-tagged Nr at the surface of unpermeabilized COS1 cells treated with or without BFA (5 µg/ml). BFA did not prevent accumulation of uncleaved Nodal precursor at the cell surface, except when *de novo* synthesis was blocked by cycloheximide (CHX, 5 µg/ml). (B) BFA inhibited the secretion of Nodal into the medium, leading to sequestration of the 47-kDa form in cell lysates.

the cysteine-rich domain (CRD) and the cytoplasmic tail of Furin did not abolish binding, suggesting that Cripto interacts with upstream sequences such as the P-domain or the catalytic domain, or both. Deletion mutants of PCs lacking the P-domain fail to undergo autocleavage and cannot exit the ER (Gluschankof and Fuller, 1994; Takahashi *et al*, 1995). Therefore, the P-domain of Furin was fused to secreted CFP (CFP-Pd), or to a signal sequence with a Flag epitope (Flag-Pd). Cripto specifically immunoprecipitated CFP-Pd (Figure 5C); conversely, Flag-Pd pulled down Cripto (Figure 5D). We conclude that Cripto independently binds the Nodal precursor and its convertases.

#### Activation of a Cripto/Nodal complex by convertases from neighbouring cells

During embryogenesis, Cripto and Nodal are coexpressed in the epiblast (Dono *et al*, 1993; Ding *et al*, 1998; Brennan *et al*, 2001; Mesnard *et al*, 2006; Figure 3A and B), whereas Furin and PACE4 are provided by extraembryonic cells (Beck *et al*, 2002; Mesnard *et al*, 2006). To mimic this configuration, 293T cells were transfected with Furin or PACE4 and co-cultured with cells expressing Nodal, Cripto and the luciferase reporter pAR3-lux (Figure 6C). We reasoned that under these conditions, exogenous PCs can only enhance Nodal signalling by cleaving precursor at the cell surface, as 293T-conditioned medium does not accumulate uncleaved Nodal precursor (Figure 6D), and because Cripto-independent cleavage barely potentiates signalling (Figure 4G and H). As a positive control, all components were transfected together in one cell population (Figure 6E). Indeed, Furin or PACE4 increased

Nodal activity 2- to 2.5-fold above endogenous levels, regardless of whether they were transfected separately or together with Nodal and Cripto. No luciferase was induced in the absence of Nodal. These results show that Furin and PACE4 activate Nodal protein that is expressed together with Cripto by neighbouring cells.

#### Cripto assembles Nodal processosomes at the cell surface

To be cleaved by extracellular PCs, Nodal may colocalize with Cripto at the plasma membrane. Immunostaining of unpermeabilized cells revealed an overlapping distribution of Cripto and cleavage-resistant Nr at the plasma membrane (Figure 6F), but the steady-state levels of wild-type precursor at the cell surface were low (Figure 6G). Although, in cells treated with the PC inhibitory peptide decanoyl-RVKR-CMK, wild-type Nodal was stabilized at the plasma membrane (Figure 6H). These results are consistent with the idea that Nodal matures at the cell surface, followed by rapid endocytosis.

To test whether Cripto recruits Nodal convertases at the plasma membrane, cells expressing Furin were co-cultured with cells producing Cripto with or without Nr. Coimmunoprecipitation analysis of chemically crosslinked cell surface proteins revealed that Furin is pulled down by Cripto together with Nodal precursor (Figure 6I). These data support a model that Cripto assembles a Nodal-processing complex at the plasma membrane.

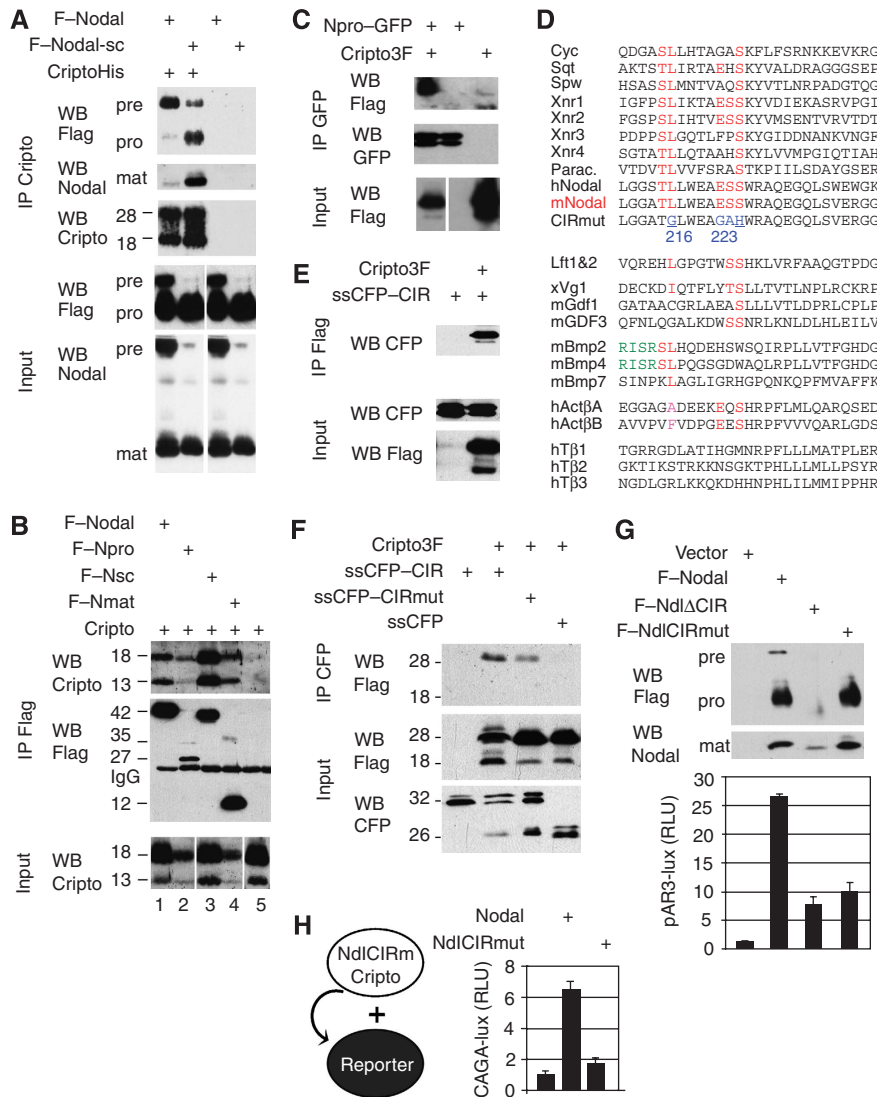


**Figure 4** Cripto binds mature and uncleaved Nodal, and a Cripto-interacting region in the propeptide ensures that Nodal processing enhances signalling. **(A)** Pull down of Flag-tagged Nodal precursor and cleaved fragments (pro, mat) by CriptoHis. Supernatant of 293T cell lines containing Nodal propeptide, mature form and residual uncleaved precursor (bottom panels, input) was incubated with metal agarose beads soaked with (lanes 1 and 2) or without (lanes 3 and 4) CriptoHis. Western blot analysis revealed that CriptoHis (18–28 kDa) precipitates Nodal precursor (pre), together with small amounts of propeptide (pro) and mature form (mat, lane 1). Mutation of the PC recognition motif RQRR/HHL to RQRR/HLE in supercleaved Nodal-sc (Constam and Robertson, 1999) increased binding of Cripto to mature Nodal and propeptide (lane 2). Mature Nodal<sub>12</sub> (12 kDa) and precursor (47 kDa) were shifted in size by 6 kDa due to an N-glycosylation site engineered to improve protein stability (Le Good *et al*, 2005). Nonspecific binding of Nodal to empty beads was below detection (lanes 3 and 4). Input samples in lanes 3 and 4 are identical to those in lanes 1 and 2, respectively. **(B)** Flag-Nodal (wild type) and Flag-Nsc precursor pulled down wild-type Cripto from detergent-soluble COS1 cell extracts (lanes 1 and 3). Cripto was also precipitated by mature Nodal (Nmat, lane 4) or propeptide (Npro, lane 2), but not in the absence of Nodal (lane 5). Lanes of input samples blotted on the same gel were cut for correct ordering. **(C)** Coimmunoprecipitation of Cripto3F with Npro-GFP fusion protein. **(D)** Residues 211–237 of the Nodal propeptide aligned with homologous sequences and other TGFβ family members. Conserved amino acids are indicated in red. Mutated residues (216–223) are indicated in blue. The most highly conserved residues of the CIR are underlined. Rose: conservative substitutions. Green: alternative PC cleavage site of proBmp2/4. **(E)** Coimmunoprecipitation of secreted CFP-CIR fusion protein with Flag-tagged Cripto. **(F)** Mutation of four conserved residues in the CIR (CIRmut) reduces Cripto binding. **(G)** In conditioned medium of transfected 293T cells, NdlΔCIR and NdlCIRmut can be processed independently of Cripto similar to wild-type Nodal (G, top panel). Below: activation of wild-type and CIR-deficient Nodal precursors in 293T cells expressing Cripto and the luciferase reporter pAR3-lux. **(H)** Mutation of the CIR also inhibits paracrine Nodal/Cripto signalling to 293T cells that were separately transfected with luciferase reporter prior to mixing with Nodal/Cripto expressing cells. Results are representative of two experiments. Error bars indicate standard deviation of triplicate values.

### Nodal matures at the cell surface and is internalized by clathrin-independent endocytic carriers

To visualize Nodal endocytosis, cells were co-transfected with Flag-tagged Nodal with or without Cripto, followed by incubation with anti-Flag antibody. Already after 5 min, internalized antibody was detectable in numerous small

foci in Nodal-transfected cells, but not in control cells, irrespective of the presence or absence of Cripto. Internalized Nodal did not colocalize with transferrin receptor, a marker of clathrin-coated early endosomes (Figure 7A), and less than 10% overlapped with known markers of clathrin-independent endocytic carriers such as GFP-



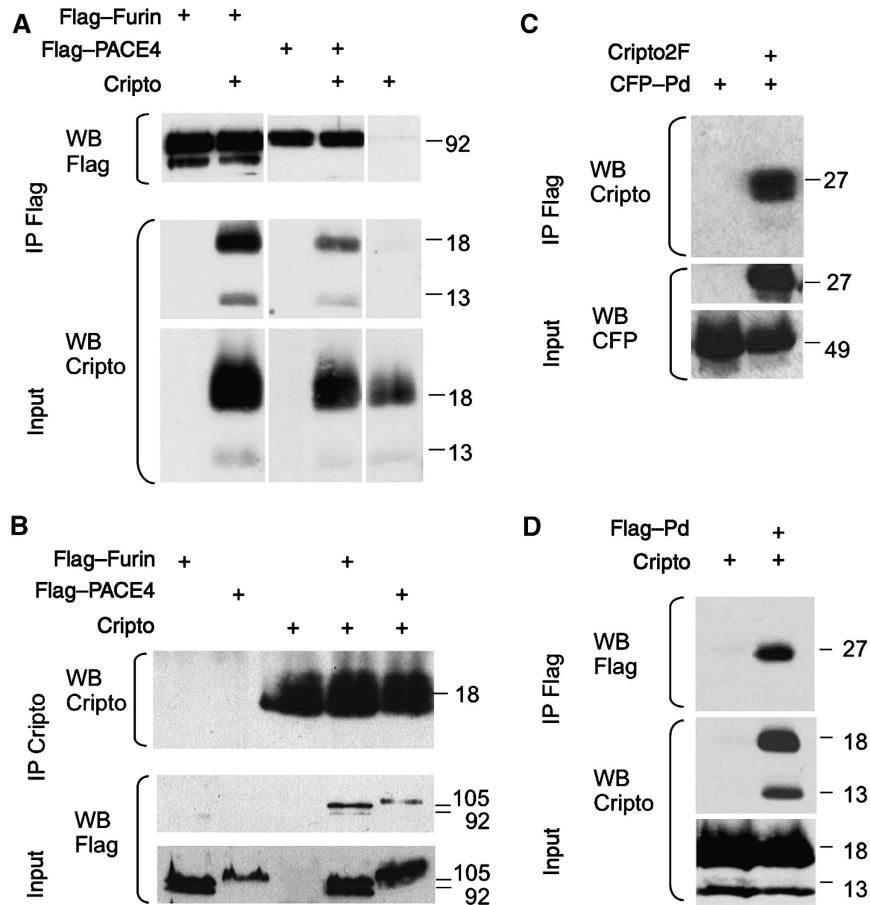


**Figure 5** Binding of Cripto to Furin and PACE4. (A) Cripto coprecipitates with Furin or PACE4, but not with control beads. Note that all samples were analysed together on the same gels, but irrelevant lanes were excised where indicated. (B) Reverse pull down of Furin and PACE4 by Cripto confirms the specificity of binding. (C, D) Coimmunoprecipitation of Cripto with the P-domain (Pd) of Furin fused to the C terminus of secreted CFP (C). For reverse pull down, the P-domain was provided with a signal sequence followed by a Flag epitope (D).

Caveolin or GFP-Flotillin (Figure 7B–D). Co-transfection of Cripto only marginally increased the overlap of internalized Nodal with GFP-Caveolin, but multiplied the percentage in GFP-Flotillin carriers by a factor of 3- to 4-fold (Figure 7D). These results suggest that Nodal is internalized by clathrin-independent routes that transiently or partially overlap with Caveolin or Flotillin (Figure 7D), and that Cripto increases the uptake or stability of Nodal in Flotillin carriers.

To validate that Nodal enters cells via clathrin-independent pathways, we also monitored antibody internalization by electron microscopy. Immunogold-labelled antibody was only detected in uncoated plasma membrane invaginations (Figure 7E). Therefore, we asked whether lipid rafts are essential for Nodal endocytosis and signalling. Disruption of rafts by the cholesterol-aggregating drug nystatin inhibited Nodal-mediated antibody uptake (Figure 7F). However, nystatin rapidly downregulated Cripto expression (Figure 7G). Therefore, we used a different approach to block Nodal uptake in rafts without depleting Cripto. To organize lipid rafts, both Caveolin and Flotillin must be palmitoylated (Morrow *et al*, 2002; Sotgia *et al*, 2002; Neumann-Giesen *et al*, 2004). Thus, if Nodal maturation and signalling rely on uptake in rafts, inhibitors of palmitoylation should block these events. Confirming this prediction, 2-bromo-palmitate (2BP) inhibited Nodal processing by endogenous convertases and by Flag-tagged Furin and PACE4. By contrast, both

proteases still accumulated in conditioned medium, indicating that 2BP did not generally inhibit protein secretion (Figure 7H). The reduction in the levels of cleaved Nodal propeptide resulting from 2BP treatment was only partially matched by a corresponding increase in uncleaved precursor (Figure 7H). This net inhibition of Nodal secretion into the medium was reminiscent of the effect of inhibitors of endosomal acidification (Supplementary Figure S2). Furthermore, antibody uptake experiments and luciferase reporter assays revealed that 2BP also inhibited Nodal endocytosis and signalling (Figure 7I). Thus, Nodal endocytosis through specific membrane microdomains is necessary for maturation and signalling.

## Discussion

Previous work has shown that Cripto activates a complex of mature Nodal with its signalling receptors. Here, we asked whether Cripto has an additional function during Nodal processing. We report that Cripto interacts with the Nodal pro segment and mature domain and presents uncleaved precursor to extracellular Furin that is recruited through its P-domain. In addition, we found that Cripto guides Nodal uptake in lipid rafts and stimulates clathrin-independent, non-caveolar endocytosis. On the basis of these results, we

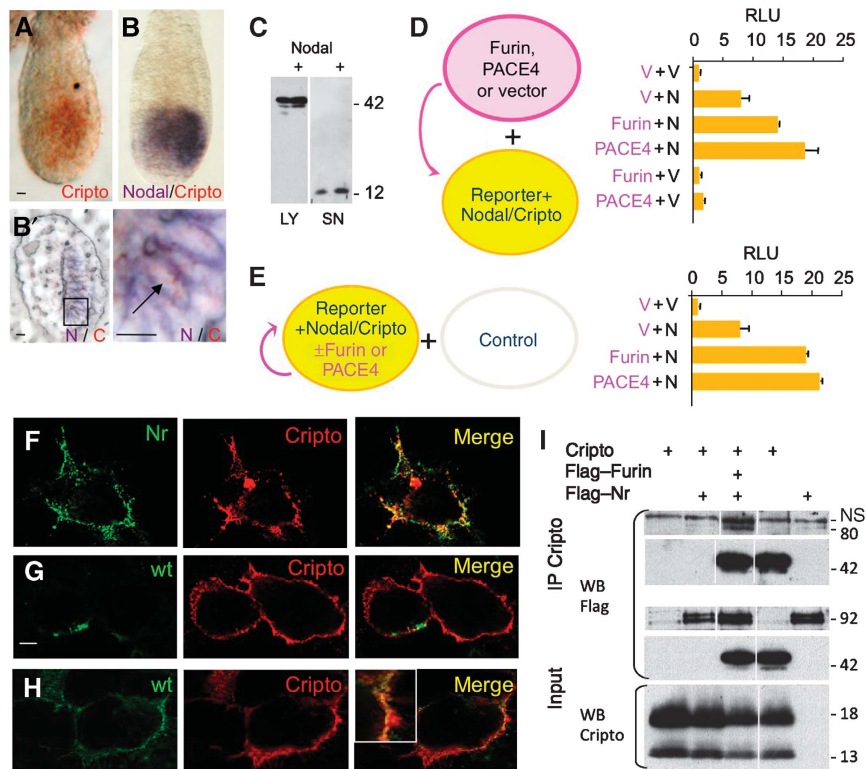


**Figure 6** A complex of Cripto and Nodal is activated in signal-receiving cells. (A, B) Whole mount view (A, B) and frozen section (B') of mouse embryos stained 6.25 days after fertilization for Cripto (A, red) and subsequently for Nodal mRNA (B, purple). Nodal and Cripto transcripts colocalize in the same cells (B'). Nodal transcripts are enriched near cell borders. Scale bars: 20  $\mu$ m. (C, D) Secreted Nodal in the medium (SN) of transiently transfected 293T cells is completely processed by endogenous PCs both with (+) or without Cripto (C). Nevertheless, induction of the Nodal luciferase reporter pAR3-lux was enhanced up to two-fold if Nodal/Cripto reporter cells were co-cultured with cells overexpressing Furin or PACE4, indicating that Nodal is likely to mature at the cell surface (D). PCs had no effect on reporter cells expressing empty vector (V). (E) For comparison, PCs, Nodal, Cripto and luciferase reporter were co-transfected into a single population of cells and co-cultured with untransfected cells. (F) Immunofluorescence analysis of non-permeabilized COS1 cells showing co-localization of Flag-Nr (green) with Cripto (red). Wild-type (wt) Flag-Nodal was less abundant at the surface of Cripto-transfected cells (G), except when cleavage was blocked by adding the PC inhibitor decanoyl-RVVKR-chloromethylketone (H). (I) Cells transfected with Flag-Furin were co-cultured for 24 h with cells expressing Cripto with or without uncleaved Nodal (Nr). The resulting complexes were reversibly crosslinked and immunoprecipitated by anti-Cripto antibody. Anti-Flag immunoblotting showed that Furin was pulled down by a complex of Cripto and uncleaved Nodal precursor. Where indicated by vertical lines, blots were cut to remove one intervening lane.

propose that Cripto couples proteolytic maturation and endocytosis of Nodal in target cells.

### **Cripto and Nodal reach the cell surface by an unconventional exocytic pathway**

Analysis of post-translational modifications of Cripto and Nodal in immunoprecipitates revealed that uncleaved Nodal binds Cripto before transit through the TGN. Furthermore, immunostaining detected both of these proteins at the cell surface even if secretion into the medium was blocked by BFA. Thus, Nodal is exposed to extracellular Furin at the cell surface without transport to the TGN and release into the medium. TGN-independent exocytosis has been described previously for the type I transmembrane protein CD45 in T lymphocytes. CD45 with immature carbohydrates is exposed at the cell surface well before sialylated isoforms (Baldwin and Ostergaard, 2002). Similarly, the EndoH-sensitive GPI-AP F3/Contactin enters lipid rafts and reaches the surface of neuroblastoma cells by a BFA-resistant route (Bonnon *et al*, 2003). Non-secretory exocytic translocation of membrane proteins is documented in neuroendocrine cells (Chiergatti and Meldolesi, 2005), but how this process is regulated is poorly understood.

### **Cripto assembles a Nodal-processing complex in signal-receiving cells**

In this study, we focused on the role of Cripto in Nodal processing. There is no evidence that Cripto stimulates Furin or PACE4 activities. However, Cripto bound the Nodal precursor and its convertases, and proNodal colocalized with Cripto and was activated in transfection assays by PCs from neighbouring cells. These results strongly support the idea that Cripto is a PC receptor. Although we examined cell-autonomous functions of Cripto, Cripto can also non-autonomously stimulate Nodal receptors in neighbouring cells (Gritsman *et al*, 1999; Yan *et al*, 2002; Chu *et al*, 2005). However, an essential role for cell non-autonomous functions of Cripto has not been demonstrated, and in zebrafish the GPI signal had to be deleted to detect this activity, suggesting that wild-type Cripto primarily functions cell-autonomously (Gritsman *et al*, 1999). Moreover, recombinant CriptoHis lacking a GPI anchor only rescued *oep* mutant embryos when injected at non-physiologically high concentrations (Minchiotti *et al*, 2001). GPI anchoring is also essential to non-autonomously stimulate Nodal/Smad2,3 signalling in cell-based assays (Watanabe *et al*, 2007; JALG, unpublished observation). Therefore, even non-autonomous



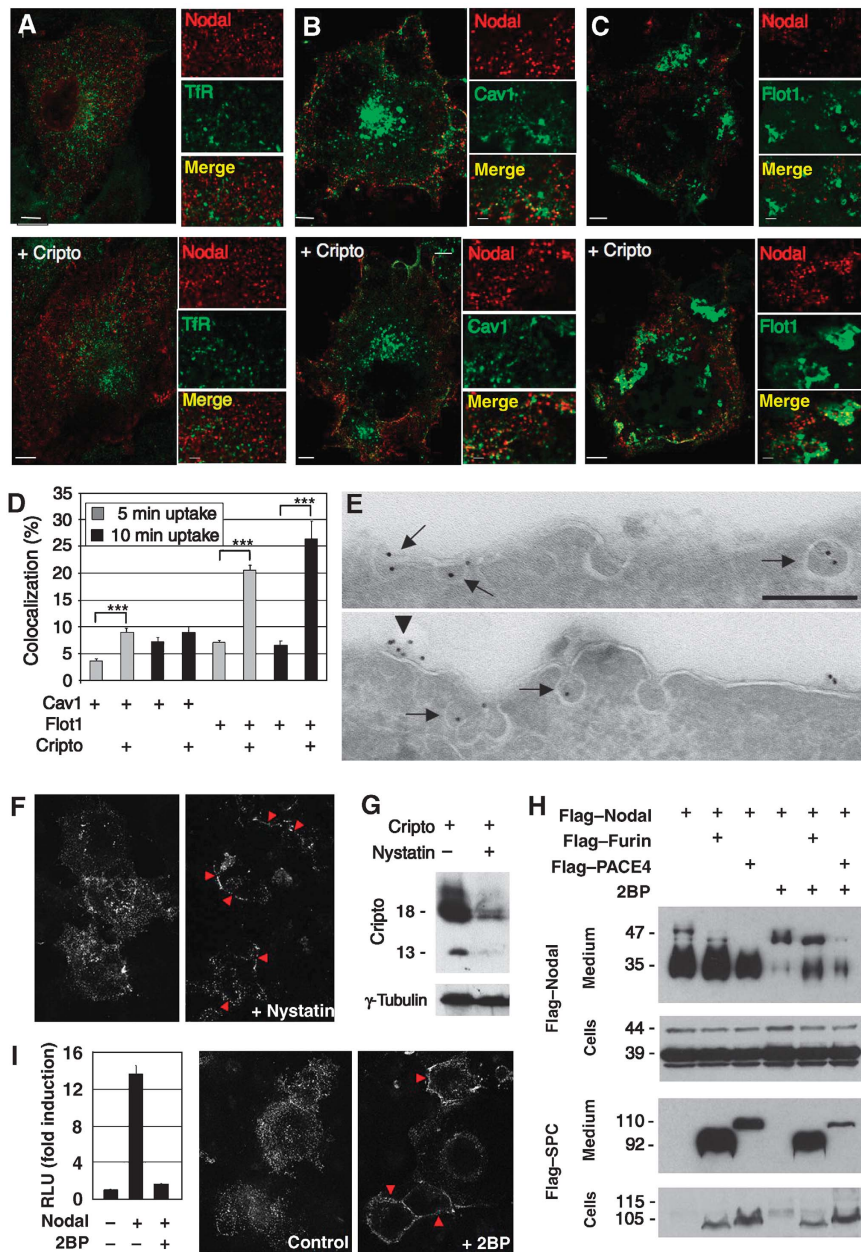


**Figure 7** Cripto recruits Nodal to nonclathrin, noncaveolar endocytic compartments marked by Flotillin-1 and -2. (A) Antibody uptake by Flag-tagged Nodal (red) in early endosomes expressing TfR was undetectable after 5 min irrespective of the presence or absence of Cripto. (B) Nodal uptake in membranes marked by GFP-Caveolin-1 in the absence and presence of Cripto. (C) Cripto mediates Nodal uptake in membranes expressing GFP-Flotillin-1. (D) Quantification of colocalization of internalized Nodal with GFP-Caveolin-1 and GFP-Flotillin-1 ( $***P < 0.001$ , Student's *t*-test). (E) Immunogold-labelled anti-Flag antibody internalized by Flag-Nodal in cells transfected with (bottom) or without Cripto (top) decorates uncoated membrane invaginations (arrows). When co-transfected with Cripto, Nodal was also detected at the surface (arrowhead). (F) Immunofluorescence staining of antibody that was internalized by Nodal in transfected COS1 cells (left panel). In cells treated with nystatin (1 h), antibody is not internalized, but instead stains the cell membrane (red arrowheads, right panel). (G) Anti-Cripto western blot of transfected COS1 treated for 4 h with or without nystatin.  $\gamma$ -Tubulin was stained as a loading control. (H) Western blot analysis of whole lysates and conditioned medium of 293T cells that were co-transfected with Cripto and the proteins indicated. Inhibition of palmitoylated proteins by 2-bromo-palmitate (2BP) reduced Nodal secretion and dramatically inhibited precursor processing by endogenous PCs and Flag-tagged Furin (lanes 1, 2, 4 and 5), and to a lesser extent exogenous Flag-PACE4 (lane 6). (I) Incubation of cells with 2-BP inhibits both Nodal signalling in a luciferase reporter assay (left panel) and Nodal-mediated antibody uptake (right panels).

effects of Cripto are likely to involve interactions with lipid microdomains of target cells.

To assess whether binding of Cripto to uncleaved Nodal is functionally relevant, we mapped a CIR in the Nodal propeptide. Mutation of four residues in this motif reduced binding to Cripto and signalling, even though Cripto-independent proteolytic processing in conditioned medium was unaf-

ected. These results support the idea that processing in a culture medium can weakly stimulate Nodal signalling, but that the CIR potentiates activation of Nodal at the plasma membrane in a complex with Cripto.

To our knowledge, Cripto is the first receptor shown to independently bind a PC and its substrate. Tissue inhibitors of metalloproteinases can mediate binding of the PACE4 and

PC5A CRDs to heparan sulphate proteoglycans (Nour *et al*, 2005), and membrane-tethered PC5/6A cleaves PCSK9 (Mayer *et al*, 2008). However, deletion of the CRD in Furin did not abolish Cripto binding, which involves the conserved P-domain.

### **Cripto stimulates Nodal uptake in Flotillin-positive membrane microdomains**

GPI-APs can be internalized by clathrin-independent carriers (Sabharanjak *et al*, 2002; Kalia *et al*, 2006) expressing the lipid raft scaffold proteins Flotillin-1 and -2 (Stuermer *et al*, 2001; Glebov *et al*, 2006). In our immunofluorescence studies, Cripto enriched Nodal in microdomains that overlapped with GFP-Flotillin, whereas Nodal alone partially or transiently localized to GFP-Caveolin carriers or unknown scavengers. This conclusion was corroborated by our electron microscopy analysis, which detected Nodal in uncoated plasma membrane invaginations both in the presence and absence of Cripto. Also in density gradients, a significant amount of Nodal was detected in detergent-resistant membranes independently of Cripto, and this proportion was further increased by Cripto. These results indicate that Cripto-mediated uptake may be required to deviate Nodal from degradative endocytic compartments during proteolytic maturation. In keeping with this model, caveolar uptake by default poises TGF $\beta$  and BMP receptors for degradation (Di Guglielmo *et al*, 2003; Satow *et al*, 2006).

The lack of Nodal uptake in clathrin-coated plasma membrane invaginations was striking. Even in cells expressing Cripto, Nodal did not directly enter early endosomes. However, exchange of cargo between clathrin-independent carriers and early endosomes has been described (Sabharanjak *et al*, 2002; Naslavsky *et al*, 2003, 2004; Sharma *et al*, 2003; Pelkmans *et al*, 2004; Kalia *et al*, 2006), and after a prolonged chase, internalized mature Nodal and its propeptide are delivered to early endosomes (M-HB, unpublished observation). Thus, we propose that Cripto-mediated Nodal uptake couples proteolytic maturation with endocytosis in signal-receiving cells. In this model, Nodal is exocytosed together with Cripto for proteolytic processing and autocrine signalling, or secreted through the TGN/endosomal system for processing in neighbouring cells. It will be interesting to determine whether Cripto also guides Nodal convertases to lipid rafts, and to identify the scaffold proteins involved. In the extracts of transfected cells, the amounts of Furin and PACE4 in detergent-resistant membranes after density gradient centrifugation were below detectable levels (M-HB, unpublished observation). It will be important, therefore, to develop more sensitive methods or biosensors that can detect PC activities in specific membrane microdomains.

## **Materials and methods**

### **Expression and immunoprecipitation of Nodal, Cripto and PCs in COS1 and 293T cells**

Cell transfection (Constam and Robertson, 1999) and immunoprecipitation assays (Yan *et al*, 2002) have been described (detailed information and a description of expression vectors are available online).

### **Detection of Nodal signalling**

Nodal activity was monitored using a luciferase assay in 293T cells (Yan *et al*, 2002). Briefly, 48 h after co-transfection with Nodal, Cripto and FoxH1, induction of the luciferase reporter AR3-lux

was measured and normalized relative to the expression of transfected  $\beta$ -galactosidase. To mimic the situation in the embryo where Nodal and its convertases are expressed in separate cell populations, cells expressing Furin, PACE4 or empty vector were mixed 24 h after transfection with separate cells expressing Cripto, FoxH1 and the AR3-lux reporter with or without Nodal. Co-cultures were lysed after 24 h to measure the induction of luciferase activity.

### **Enzymatic removal of carbohydrates**

Immunoprecipitated Cripto was incubated with N-glycosidase F or EndoH (Roche) for 1 h at 37°C in 50 mM sodium phosphate buffer pH 5.5. De-glycosylated proteins were dissolved in SDS sample buffer and analysed by immunoblotting.

### **Immunofluorescent staining of permeabilized and non-permeabilized cells**

To visualize the localization of Nodal and Cripto, cells transfected on coverslips were fixed in 4% paraformaldehyde for 15 min. Where indicated, cells were permeabilized with 0.02% Triton X-100 followed by indirect immunofluorescence analysis using fluorescein- or Cy3-coupled secondary anti-mouse or anti-rabbit antibodies at the recommended concentrations (Molecular Probes). Cell surface expression of Nodal and Cripto on non-permeabilized cells was detected using anti-Flag M2 or anti-Cripto C terminus antibody (dilution 1:400). For antibody uptake, transfected cells were incubated at 37°C for the indicated time in a culture medium containing 9  $\mu$ g/ml anti-Flag M2 antibody. After washing with PBS, cells were fixed, permeabilized and stained as described above using Cy3-anti-mouse antibody. Stained coverslips were mounted in DABCO mounting medium and analysed by confocal microscopy (Zeiss LSM 510).

### **Transmission electron microscopy**

Electron microscopy was conducted as described online in Supplementary data.

### **Double whole mount *in situ* hybridization**

Embryos were dissected 6.5 days post-coitum and fixed overnight at 4°C in PBS containing 4% paraformaldehyde and 0.1% v/v Tween-20. DIG-labelled Nodal and fluorescein-labelled Cripto antisense mRNA probes were hybridized to whole mount embryos and sequentially revealed using BM purple and INT/BCIP to detect alkaline phosphatase conjugated to anti-DIG and anti-FLUO antibodies (Roche), respectively. Frozen sections (8  $\mu$ m) were obtained after embedding stained embryos in glycerol containing 30% (w/v) sucrose.

### **Density fractionation gradients**

All of the following steps were performed in the cold room. At 48 h after transfecting  $6 \times 10^5$  COS1 cells, cells were incubated for 30 min on ice in 200  $\mu$ l TNE buffer (25 mM Tris-HCl pH 7.4, 150 mM NaCl, 5 mM EDTA) containing protease inhibitors (Complete Mini, Roche) and 1% Triton X-100. The resulting cell suspensions were passed 10 times through a 26G needle, and protein concentrations were adjusted to 1.2  $\mu$ g/ml. Of the resulting homogenates, 90  $\mu$ l was thoroughly mixed with 120  $\mu$ l of 60% Optiprep (stock solution; Axon Lab) and then overlaid without mixing by 2 ml of 30% Optiprep (diluted in TNE) and 190  $\mu$ l of TNE buffer. After centrifugation for 2 h (55 000 r.p.m., 25 9000  $\times$  g at 4°C), six 400  $\mu$ l fractions were precipitated by adding sodium deoxycholate (125  $\mu$ g/ml) and trichloroacetic acid (4.8 mg/ $\mu$ l). After resuspension in SDS sample buffer, proteins of interest were visualized in each fraction by western blot analysis.

### **Supplementary data**

Supplementary data are available at *The EMBO Journal* Online (<http://www.embojournal.org>).

## **Acknowledgements**

The influence of Cripto on Nodal trafficking was characterized by M-HB; JALG and SB elucidated protein-protein interactions. Double *in situ* hybridizations were conducted by DM, whereas VO and JK analysed Nodal endocytosis by immunogold labelling

and electron microscopy. GM provided anti-Cripto antibody and Cripto expression vectors. DBC constructed expression vectors and wrote the paper. We are grateful to M Whitman for providing ALK4, Cripto and FoxH1 expression vectors, and to G van der Goot for helpful discussions. M-HB and JALG were supported by the Swiss Cancer League (grant KLS-01301-02-2003).

## References

- Anderson ED, Molloy SS, Jean F, Fei H, Shimamura S, Thomas G (2002) The ordered and compartment-specific autoproteolytic removal of the furin intramolecular chaperone is required for enzyme activation. *J Biol Chem* **277**: 12879–12890
- Baldwin TA, Ostergaard HL (2002) The protein-tyrosine phosphatase CD45 reaches the cell surface via Golgi-dependent and -independent pathways. *J Biol Chem* **277**: 50333–50340
- Beck S, Le Good JA, Guzman M, Haim NB, Roy K, Beermann F, Constam DB (2002) Extraembryonic proteases regulate Nodal signalling during gastrulation. *Nat Cell Biol* **4**: 981–985
- BenHaim N, Lu C, Pescatore L, Mesnard D, Bischofberger M, Naef F, Robertson EJ, Guzman M, Constam DB (2006) The Nodal precursor acting via activin receptors induces mesoderm by maintaining a source of its convertases and BMP4. *Dev Cell* **11**: 1–11
- Bianco C, Kannan S, De Santis M, Seno M, Tang CK, Martinez-Lacaci I, Kim N, Wallace-Jones B, Lippman ME, Ebert AD, Wechselberger C, Salomon DS (1999) Cripto-1 indirectly stimulates the tyrosine phosphorylation of erb B-4 through a novel receptor. *J Biol Chem* **274**: 8624–8629
- Bonnon C, Goutebroze L, Denisenko-Nehrbass N, Girault JA, Favre-Sarrahil C (2003) The paranodal complex of F3/contactin and caspr/paranodin traffics to the cell surface via a non-conventional pathway. *J Biol Chem* **278**: 48339–48347
- Brennan J, Lu CC, Norris DP, Rodriguez TA, Beddington RS, Robertson EJ (2001) Nodal signalling in the epiblast patterns the early mouse embryo. *Nature* **411**: 965–969
- Chapman RE, Munro S (1994) Retrieval of TGN proteins from the cell surface requires endosomal acidification. *EMBO J* **13**: 2305–2312
- Chen C, Shen MM (2004) Two modes by which Lefty proteins inhibit nodal signaling. *Curr Biol* **14**: 618–624
- Chen C, Ware SM, Sato A, Houston-Hawkins DE, Habas R, Matzuk MM, Shen MM, Brown CW (2006) The Vg1-related protein Gdf3 acts in a Nodal signaling pathway in the pre-gastrulation mouse embryo. *Development* **133**: 319–329
- Cheng SK, Olale F, Bennett JT, Brivanlou AH, Schier AF (2003) EGF-CFC proteins are essential coreceptors for the TGF-beta signals Vg1 and GDF1. *Genes Dev* **17**: 31–36
- Chiergatti E, Meldolesi J (2005) Regulated exocytosis: new organelles for non-secretory purposes. *Nat Rev Mol Cell Biol* **6**: 181–187
- Chu J, Ding J, Jeays-Ward K, Price SM, Placzek M, Shen MM (2005) Non-cell-autonomous role for Cripto in axial midline formation during vertebrate embryogenesis. *Development* **132**: 5539–5551
- Constam DB, Robertson EJ (1999) Regulation of bone morphogenetic protein activities by pro domains and proprotein convertases. *J Cell Biol* **144**: 139–149
- Di Guglielmo GM, Le Roy C, Goodfellow AF, Wrana JL (2003) Distinct endocytic pathways regulate TGF-beta receptor signalling and turnover. *Nat Cell Biol* **5**: 410–421
- Ding J, Yang L, Yan YT, Chen A, Desai N, Wynshaw-Boris A, Shen MM (1998) Cripto is required for correct orientation of the anterior-posterior axis in the mouse embryo. *Nature* **395**: 702–707
- Dono R, Scalera L, Pacifico F, Acampora D, Persico MG, Simeone A (1993) The murine cripto gene: expression during mesoderm induction and early heart morphogenesis. *Development* **118**: 1157–1168
- Fivaz M, Vilbois F, Thurnheer S, Pasquali C, Abrami L, Bickel PE, Parton RG, van der Goot FG (2002) Differential sorting and fate of endocytosed GPI-anchored proteins. *EMBO J* **21**: 3989–4000
- Glebov OO, Bright NA, Nichols BJ (2006) Flotillin-1 defines a clathrin-independent endocytic pathway in mammalian cells. *Nat Cell Biol* **8**: 46–54
- JALG was also a recipient of the Human Frontiers Science Program postdoctoral fellowship LT00360/2001-M. DM and DBC are funded by the Swiss National Science Foundation (grants 3100-062031.00 and 3100A0-105583/1), GM is funded by Associazione Italiana Ricerca sul Cancro (AIRC).
- Gluschankof P, Fuller RS (1994) A C-terminal domain conserved in precursor processing proteases is required for intramolecular N-terminal maturation of pro-Kex2 protease. *EMBO J* **13**: 2280–2288
- Gritsman K, Zhang J, Cheng S, Heckscher E, Talbot WS, Schier AF (1999) The EGF-CFC protein one-eyed pinhead is essential for nodal signaling. *Cell* **97**: 121–132
- Guzman M, Ben-Haim N, Beck S, Constam DB (2004) Nodal protein processing and fibroblast growth factor-4 synergize to maintain a trophoblast stem cell microenvironment. *Proc Natl Acad Sci USA* **101**: 15656–15660
- Kalia M, Kumari S, Chadda R, Hill MM, Parton RG, Mayor S (2006) Arf6-independent GPI-anchored protein-enriched early endosomal compartments fuse with sorting endosomes via a Rab5/phosphatidylinositol-3'-kinase-dependent machinery. *Mol Biol Cell* **17**: 3689–3704
- Kenney NJ, Smith GH, Maroulakou IG, Green JH, Muller WJ, Callahan R, Salomon DS, Dickson RB (1996) Detection of amphiregulin and Cripto-1 in mammary tumors from transgenic mice. *Mol Carcinog* **15**: 44–56
- Le Good JA, Joubin K, Giraldez AJ, Ben-Haim N, Beck S, Chen Y, Schier AF, Constam DB (2005) Nodal stability determines signaling range. *Curr Biol* **15**: 1–20
- Liguori GL, Borges AC, D'Andrea D, Liguoro A, Goncalves L, Salgueiro AM, Persico MG, Belo JA (2008) Cripto-independent Nodal signaling promotes positioning of the A-P axis in the early mouse embryo. *Dev Biol* **315**: 280–289
- Mallet WG, Maxfield FR (1999) Chimeric forms of furin and TGN38 are transported with the plasma membrane in the trans-Golgi network via distinct endosomal pathways. *J Cell Biol* **146**: 345–359
- Mayer G, Hamelin J, Asselin MC, Pasquato A, Marcinkiewicz E, Tang M, Tabibzadeh S, Seidah NG (2008) The regulated cell surface zymogen activation of the proprotein convertase PC5A directs the processing of its secretory substrates. *J Biol Chem* **283**: 2373–2384
- Mesnard D, Guzman-Ayala M, Constam DB (2006) Nodal specifies embryonic visceral endoderm and sustains pluripotent cells in the epiblast before overt axial patterning. *Development* **133**: 2497–2505
- Minchiotti G, Manco G, Parisi S, Lago CT, Rosa F, Persico MG (2001) Structure-function analysis of the EGF-CFC family member Cripto identifies residues essential for nodal signalling. *Development* **128**: 4501–4510
- Morrow IC, Rea S, Martin S, Prior IA, Prohaska R, Hancock JF, James DE, Parton RG (2002) Flotillin-1/reggie-2 traffics to surface raft domains via a novel Golgi-independent pathway. Identification of a novel membrane targeting domain and a role for palmitoylation. *J Biol Chem* **277**: 48834–48841
- Naslavsky N, Weigert R, Donaldson JG (2003) Convergence of non-clathrin- and clathrin-derived endosomes involves Arf6 inactivation and changes in phosphoinositides. *Mol Biol Cell* **14**: 417–431
- Naslavsky N, Weigert R, Donaldson JG (2004) Characterization of a nonclathrin endocytic pathway: membrane cargo and lipid requirements. *Mol Biol Cell* **15**: 3542–3552
- Nebenfuhr A, Ritzenthaler C, Robinson DG (2002) Brefeldin A: deciphering an enigmatic inhibitor of secretion. *Plant Physiol* **130**: 1102–1108
- Neumann-Giesen C, Falkenbach B, Beicht P, Claassen S, Luers G, Stuermer CA, Herzog V, Tikkanen R (2004) Membrane and raft association of reggie-1/flotillin-2: role of myristoylation, palmitoylation and oligomerization and induction of filopodia by overexpression. *Biochem J* **378**: 509–518
- Nour N, Mayer G, Mort JS, Salvat A, Mbikay M, Morrison CJ, Overall CM, Seidah NG (2005) The cysteine-rich domain of the secreted proprotein convertases PC5A and PACE4 functions as a

- cell surface anchor and interacts with tissue inhibitors of metalloproteinases. *Mol Biol Cell* **16**: 5215–5226
- Pelkmans L, Burli T, Zerial M, Helenius A (2004) Caveolin-stabilized membrane domains as multifunctional transport and sorting devices in endocytic membrane traffic. *Cell* **118**: 767–780
- Pezeron G, Lambert G, Dickmeis T, Strahle U, Rosa FM, Mourrain P (2008) Rasl11b knock down in zebrafish suppresses one-eyed-pinhead mutant phenotype. *PLoS ONE* **3**: e1434
- Piek E, Van Dinther M, Parks WT, Sallee JM, Bottinger EP, Roberts AB, Ten Dijke P (2004) RLP, a novel Ras-like protein, is an immediate-early transforming growth factor-beta (TGF-beta) target gene that negatively regulates transcriptional activity induced by TGF-beta. *Biochem J* **383**: 187–199
- Reissmann E, Jornvall H, Blokzijl A, Andersson O, Chang C, Minchiotti G, Persico MG, Ibanez CF, Brivanlou AH (2001) The orphan receptor ALK7 and the Activin receptor ALK4 mediate signaling by Nodal proteins during vertebrate development. *Genes Dev* **15**: 2010–2022
- Sabharanjak S, Sharma P, Parton RG, Mayor S (2002) GPI-anchored proteins are delivered to recycling endosomes via a distinct cdc42-regulated, clathrin-independent pinocytic pathway. *Dev Cell* **2**: 411–423
- Satow R, Kurisaki A, Chan TC, Hamazaki TS, Asashima M (2006) Dullard promotes degradation and dephosphorylation of BMP receptors and is required for neural induction. *Dev Cell* **11**: 763–774
- Schier AF (2003) Nodal signaling in vertebrate development. *Annu Rev Cell Dev Biol* **19**: 589–621
- Sharma DK, Choudhury A, Singh RD, Wheatley CL, Marks DL, Pagano RE (2003) Glycosphingolipids internalized via caveolar-related endocytosis rapidly merge with the clathrin pathway in early endosomes and form microdomains for recycling. *J Biol Chem* **278**: 7564–7572
- Shen MM (2007) Nodal signaling: developmental roles and regulation. *Development* **134**: 1023–1034
- Sotgia F, Razani B, Bonucci G, Schubert W, Battista M, Lee H, Capozza F, Schubert AL, Minetti C, Buckley JT, Lisanti MP (2002) Intracellular retention of glycosylphosphatidylinositol-linked proteins in caveolin-deficient cells. *Mol Cell Biol* **22**: 3905–3926
- Stuermer CA, Lang DM, Kirsch F, Wiechers M, Deininger SO, Plattner H (2001) Glycosylphosphatidylinositol-anchored proteins and fyn kinase assemble in noncaveolar plasma membrane microdomains defined by reggie-1 and -2. *Mol Biol Cell* **12**: 3031–3045
- Takahashi S, Nakagawa T, Kasai K, Banno T, Duguay SJ, Van de Ven WJ, Murakami K, Nakayama K (1995) A second mutant allele of furin in the processing-incompetent cell line, LoVo. Evidence for involvement of the homo B domain in autocatalytic activation. *J Biol Chem* **270**: 26565–26569
- Thomas G (2002) Furin at the cutting edge: from protein traffic to embryogenesis and disease. *Nat Rev Mol Cell Biol* **3**: 753–766
- Watanabe K, Hamada S, Bianco C, Mancino M, Nagaoka T, Gonzales M, Bailly V, Strizzi L, Salomon DS (2007) Requirement of glycosylphosphatidylinositol anchor of cripto-1 for 'trans' activity as a nodal co-receptor. *J Biol Chem* **282**: 35772–35786
- Yan YT, Liu JJ, Luo Y, Chaosu E, Haltiwanger RS, Abate-Shen C, Shen MM (2002) Dual roles of Cripto as a ligand and coreceptor in the nodal signaling pathway. *Mol Cell Biol* **22**: 4439–4449